RAVEN: The Low-Latency Gravitational Wave Focused Multi-messenger Search

B. J. Piotrzkowski [1] N. Adhikari [1] V. Gayathri [1] G. Waratkar [2] A. M. Toivonen [3]
M. Cho,[4] Shaon Ghosh [5] S. Sharma-Chaudhary,[6] P. R. Brady [1] E. Katsavounidis,[7]
M. W. Coughlin [3] V. Bhalero [2] T. Dal Canton [8] S. Bose,[9] and A. M. Sintes [10]

[1] University of Wisconsin-Milwaukee, Milwaukee, WI 53201, USA
[2] Department of Physics, Indian Institute of Technology Bombay, Powai, 400 076, India
[3] University of Minnesota, Minneapolis, MN 55455, USA
[4]
[5] Montclair State University, Montclair, NJ 07043, USA
[6] Missouri University of Science and Technology, Rolla, MO 65409, USA
[7] LIGO Laboratory, Massachusetts Institute of Technology, Cambridge, MA 02139, USA
[8] Université Paris-Saclay, CNRS/IN2P3, IJCLab, 91405 Orsay, France
[9] Washington State University, Pullman, WA 99164, USA
[10] IAC3–IEEC, Universitat de les Illes Balears, E-07122 Palma de Mallorca, Spain

We discuss the Rapid, on-source VOEvent Coincident Monitor (RAVEN), a low-latency gravitational wave-focused multi-messenger search pipeline adopted by the LIGO-Virgo-KAGRA (LVK) collaboration. RAVEN has been in operation searching for multi-messenger GW-GRB signals since the second observing run (O2), assisting in the prompt joint detection of GW170817-GRB 170817A [1–5]. In this paper, we describe the RAVEN search method, as well as the manner of assigning significance and sending alerts. We discuss the performance of these methods using Mock Data Challenge results along with simulated data analysis. RAVEN plays an important role in multi-messenger astronomy in O4 and beyond, facilitating rapid electromagnetic follow-up and potentially finding crucial new multi-messenger events.

I. INTRODUCTION

With the coincident detection of the binary neutron star (BNS) gravitational wave (GW) signal GW170817 and gamma-ray burst GRB 170817A [2, 6–8], multi-messenger astronomy with gravitational waves squarely entered the realm of observational science. This detection was found rather early by the multi-messenger pipeline referred to as the Rapid, on-source VOEvent Coincident Monitor (RAVEN), internally alerting the LIGO-Virgo-KAGRA collaboration (LVK; [9–12]) of this coincidence within a latency of 6 seconds after being called and 7 minutes after the GW merger [13]. Initial localizations were later provided by *Fermi*-GBM (delay of 25 min; [14]), and then by the LVK first using both the Hanford and Livingston GW detectors (delay of 50 min; [15]), and then later including the Virgo detector (delay of 4.5 hours). This prompt detection and the subsequent localization led to the detection of the optical transient kilonova AT 2017gfo, announced around 11 hours after the merger [16, 17].

Since GW170817, the astronomy community receiving these GW alerts for follow-up observations across the electromagnetic wavelengths have tremendously improved the latencies of their observations. Several X-ray transient monitors like *Fermi*-GBM, *Swift*-BAT, *INTEGRAL*, *KONUS*-Wind, *AstroSat*-CZTI, *AGILE*, which regularly undertake deep archival searches typically at the end of observing runs [18–23], have also setup automated low-latency sub-threshold searches following these GW alerts. In other wavelengths, several observatories have set up infrastructure which can trigger follow-up telescopes within seconds to minutes of the GW alert going out [24–26]. Such rapid follow-up observations could help us understand the early rise of the optical light curve which can give stronger constraint on kilonova models [27]. Further, there has been a tremendous effort to reduce the latency of the LVK GW alert system. At the moment of writing, the total delay from the merger time to sending an alert is 30 s or less [28], which is much lower than the latencies observed in the previous observing runs [29]. Further, ith several instances of early warning alerts of BNS merger candidates already reported [30].

RAVEN has also received separate major improvements, now being able to autonomously send alerts of coincident events and analyze sub-threshold GRBs with all GW events. RAVEN now has two primary functions: i.) find and determine the significance of GW events coincident with GRBs or neutrino bursts, including *sub-threshold* GW events, which could be of interest to the astronomical community and ii.) alert the external astronomical community and deliver data products in a latency low enough to facilitate electromagnetic follow-up. RAVEN can identify additional GW candidates via their temporal proximity to external astrophysical transients and agreement in sky localizations.

In this paper, we will outline the design of RAVEN as a part of the LVK low-latency infrastructure in section II, describe how RAVEN assigns significance to joint coincident candidates in section III, present the results of simulations for this analysis in section IV, discuss the latencies of this system in V, and conclude with a discussion in VI.

II. RAVEN PIPELINE DESIGN

The RAVEN pipeline is built as a module in `gwcelery` [31], the hub of the LVK low-latency analysis, and uses a few simple functions from the standalone python package *ligo-raven*[32]. `gwcelery` helps trigger RAVEN whenever there is any new GW superevent or any updates to the existing superevent as described below, and also helps update these superevents on GraceDB[33] if the publishing criteria are met. The RAVEN package consists primarily of three functions: i.) a query of the Gravitational-Wave Candidate Event Database (GraceDB) to look for coincident GW events and external events within a given time window, ii.) a calculation of the joint significance using Equation (1) or (10) depending on the type of search, and iii.) a calculation of the overlap between sky maps if they are available, described later in Section III.

The basic design of the RAVEN pipeline is to perform queries of the GraceDB database whenever either a GW event or an external event is uploaded to GraceDB. The collection of data concerning a single GW candidate is organized into a superevent in GraceDB, which includes triggers from the various GW pipelines within a narrow time window (usually [-1,+1] s), while an external event is created after receiving a Gamma-ray Coordination Network (GCN) VOEvent [34] or Kafka JSON notice [35]. The query in GraceDB checks whether there is a complementary event within a predetermined coincidence time window, chosen based on both the type of event queried on and being searched for as seen in table I. If a coincident event is found, a set of publishing conditions are then checked and, if met, an automatic alert is sent out via a GCN notice. See Figure 1 for a detailed flowchart of this pipeline and sections III C and III D for the full set of publishing conditions. Additionally, the *ligo-raven* package is user-friendly and can be used to run rapid offline searches, using any combination of online GraceDB instances or local CSV files.

Updates to the state of either the external event or GW superevent in a known coincidence can trigger additional functionality. The RAVEN pipeline is re-run whenever any of the following conditions are met — either the superevent and external events gets updated with new sky maps, whenever either of their existing sky maps are updated, or whenever a different GW pipeline candidate is chosen to represent the superevent (i.e. the preferred event changes). If the external event was previously flagged as likely non-astrophysical and this flag is later removed through an update from the respective experiment, we re-run the RAVEN pipeline and check whether the publishing criteria are met.

Since O3, RAVEN has listened for GRB candidates via GCN from *Fermi*-GBM [36], *Swift*-BAT [37], INTEGRAL [38], and *AGILE*-MCAL [39] up to its point of decommissioning. RAVEN has also listened to neutrino burst candidates from SNEWS [40]. From the beginning of O4a, *Fermi* and *Swift* have also participated in an additional sub-threshold search described in III B. Participating compact binary coalescence (CBC) focused GW pipelines include GstLAL [41], PyCBC [42], MBTAOnline [43], and SPIIR [44]. The cWB pipeline also participates, searching for unmodeled GW transients [45] and binary black hole candidates [46].

RAVEN ran using its query functionality during the entirety of O3, while the ability to send alerts and use sky maps was added later in O3b. By O4, a number of new improvements were made. The algorithm to compare sky maps was expanded to handle multi-ordered coverage [MOC; ?] sky maps, leading up to a 10x decrease in latency for this calculation. The targeted search described in section III B was finished and began producing candidates. The ability to switch the external event listed in the alert was added, preferring the one with the highest significance. Automatic periodic end-to-end testing of all the various searches was added to ensure the system is always working as expected, as discussed in V, alongside the existing rounds of manual review and built-in pytests. The performance in O4 has been stable and reliable to the point where human intervention has not been needed up to the time of writing, a frequent occurrence in O3 and before.

III. JOINT SIGNIFICANCE

Research on the joint significance of multi-messenger events has been ongoing, motivated by finding more coincidences that may be less significant than GW170817-GRB 170817A. To this aim, various joint ranking statistics such as odds ratios and Bayes factors have been employed in searches. However, these methods often require complete datasets to compare signals against the background, making them more suitable for offline analysis [47–49]. For low-latency searches like RAVEN, the false alarm rate (FAR) is a more practical statistic, as it compares against the *immediate* surrounding background that is readily available. The LVK already utilizes FARs to evaluate the significance of gravitational-wave candidates in noise-dominated data [50]. In multi-messenger searches, the key metric of interest is the false alarm rate of the joint coincident event, rather than that of the individual candidates. Although a joint candidate with a low FAR may indicate statistical significance, it does not necessarily imply that physically meaningful parameters can be inferred through parameter estimation. Moreover, a low joint FAR does not guarantee an astrophysical association between the two candidates, which is the primary purpose of the coincidence odds ratio [47, 51]. A low joint FAR means that a similar false joint candidate does not occur often and likely should be of interest for additional follow-up, due to one or both of the candidates likely being real.

RAVEN has two methods of assigning joint significance, separated into an untargeted method described in section III A and a targeted method in section III B. The untargeted method involves taking in both streams of GW events and external events independently, performing queries when either is ingested. The targeted method instead requires sending moderately significant GW events (with FARs of less than two per day) to external partners, such as Fermi, AGILE, INTEGRAL and *Swift*, where they then search their sub-threshold data for possible coincidence. If a coincidence is found, the corresponding GRB candidate is sent back and ingested similarly to the targeted search. These methods are also differentiated by the nature of the GRB candidates considered. The untargeted method considers highly significant GRBs while the targeted considers lower significance GRBs well in the sub-threshold regime. This is reflected in the term dominating the rates of GRB candidates used, with the expected detectable rate of astrophysical GRBs being used in eqn (1) and the FAR reported by the GRB pipeline in eqn (10).

Search	Pipeline(s)	Untargeted	Targeted
GW CBC-GRB	Fermi/GBM	[-1, +5]	[-1, +11]
	Swift/BAT	[-1, +5]	[-10, +20]
	INTEGRAL	[-1, +5]	N/A
	AGILE	[-1, +5]	N/A
GW Burst-GRB	Fermi/GBM	[-60, +600]	[-1, +11]
	Swift/BAT	[-60, +600]	[-10, +20]
	INTEGRAL	[-60, +600]	N/A
	AGILE	[-60, +600]	N/A
GW Burst-Neutrino	SNEWS	[-10, +10]	N/A

TABLE I: Coincident time windows in seconds chosen based on search and pipeline, centered on the GW merger/burst time. Wider windows were chosen for GW bursts due to the lack of confident tight delay models for GRBs from supernova and other progenitors of GW bursts [52]. Slightly wider windows were chosen for the targeted searches in order to include models that predict additional delay [52], with *Swift* being confident to rule out noise events due to their highly precise localizations. The tighter window for SNEWS compensates for the time delay due to the mass of neutrinos emitted just outside our galaxy.

A. Untargeted GW-GRB Analysis

The test statistic used in the untargeted analysis that we assert is the joint FAR (FAR_c), first derived in [53] and then modified in [54], is

$$FAR_c = FAR_{gw} \frac{R_{ext} \Delta t}{\mathcal{I}_\Omega} \tag{1}$$

where FAR_{gw} is the FAR given by one of the GW pipelines, R_{ext} is the rate of unique external candidates in a given search (e.g. GRBs), Δt is the total coincident time window, and $\mathcal{I}_\Omega$ is the sky map overlap integral [47]. The coincident time window is chosen based on the event and desired search, described in table I. The rate of GRBs here has been measured as $310/yr$ after considering joint detections between GRB experiments [53, 55–58], shown in table II. The external candidates considered here are highly significant, except for sub-threshold Fermi GBM candidates with an additional rate of $65/yr$, and are all published via GCN prior to being processed by RAVEN [59]. We note these sub-threshold GRBs are still significant compared to the background, where filtering based on classification helps rule most of the noise transients out so we still expect the real detection rate to dominate.

The sky map overlap integral in eqn (1), first defined in [47], can be written as

$$\mathcal{I}_\Omega(x_{gw}, x_{ext}) = \int \frac{p(\Omega|x_{gw}, \mathcal{H}^s_{gw}) p(\Omega|x_{ext}, \mathcal{H}^s_{ext})}{p(\Omega|\mathcal{H}^s)} d\Omega \tag{2}$$

where $\mathcal{H}^s_a$ is the hypothesis that the data x_a is from a real astrophysical signal, $p(\Omega|x_a, \mathcal{H}^s_a)$ is the normalized probability density of the event a at coordinates Ω, and $p(\Omega|\mathcal{H}^s)$ is the prior on sky position, which we take as uniform so that $p(\Omega|\mathcal{H}^s) = 1/4\pi$. This uniform prior could likely be improved by considering the sensitivity of the experiments involved at the time of detection. To compute eqn (2) with Hierarchical Equal Area iso-Latitude Pixelization of a sphere (HEALPix) sky maps [60, 61], we can subdivide the sky into pixels with equal area $d\Omega \approx \Delta A$ as in [54]. We denote each pixel by the index i so that $p(\Omega|x_a, \mathcal{H}^s_a)\Delta A \approx P(i|x_a, \mathcal{H}^s_a)$ and $4\pi \cdot p(\Omega|x_a, \mathcal{H}^s_a) \approx N_{pix} \cdot P(i|x_a, \mathcal{H}^s_a)$, where $p(\Omega)$ is probability density at coordinate Ω and $P(i)$ is the probability in pixel i. This all together yields

$$\mathcal{I}_\Omega(x_{gw}, x_{ext}) \approx N_{pix} \sum_{i=1}^{N_{pix}} P(i|x_{gw}, \mathcal{H}^s_{gw}) P(i|x_{ext}, \mathcal{H}^s_{ext}) \tag{3}$$

where we have assumed each sky map has the same resolution with N_{pix} being the number of pixels in a single sky map.

However, we typically compute eqn (2) for multi-ordered-coverage (MOC) sky maps, which vary their resolution to put more points near areas of higher probability density, and use the *uniq* indexing scheme

$$uniq = i_{pix} + 4\ nside^2 \tag{4}$$

where i_{pix} is the standard HEALPix index with resolution $nside$. This presents a challenge of computing the sky map overlap integral from eqn (3), since the indices of two sky maps would no longer trivially match. Fortunately, the coordinates (i.e. right ascension and declination) allow us to match pixels of sky maps with any resolution or configuration. Therefore we developed the following algorithm for handling MOC sky maps

1. For the first sky map, convert the *uniq* index into nside ($nside_1 = 2^{\lfloor \log_2(uniq_1/4)/2 \rfloor}$) and then to pixel

Search	Pipeline(s)	R_{ext}	$FAR_{gw,max}$	$FAR_{ext,max}$
GRB	Fermi/GBM	+235/yr		
	Swift/BAT	+65/yr		
	INTEGRAL	+5/yr		
	AGILE	+5/yr		
	Total	310/yr		
SubGRB	Fermi/GBM	+65/yr		
	Total	375/yr		
SubGRBTargeted	Fermi/GBM		2/day	1/10000 s
	Swift/BAT		2/day	1/1000 s
Supernova	SNEWS		1/day	

TABLE II: Rates used in eqn (1) and eqn (10) for the various searches and pipelines. Note that the total rates for R_{ext} are used rather than the individual contributing rates. The rate for AGILE was removed after it was decommissioned around the start of O4b. The SubGRB rates are added to the total GRB rate since they should be less significant. The two SubGRBTargeted pipelines are considered separate due to their different time windows and potential different emission models. The rate shown for the SNEWS search is simply the threshold to publish that the GW candidate must be more significant, rather than using either of the joint FAR methodologies.

area ($\Delta A_1 = 4\pi/N_{pix,1}$ where the total number of pixels $N_{pix,1} = 12\ nside_1^2$) [62].

2. Find the coordinates Ω_1 (RA, dec) of a given pixel using the index ($i_1 = uniq - 4nside^2$) [63].

3. Compute the coordinates of the second sky map Ω_2 and then find the closest corresponding pixel where $\Omega_2 \approx \Omega_1$.

With each pixel in the first sky map matched to another in the second, the sky map overlap can be computed as

$$I_\Omega(x_1, x_2) \approx 4\pi \sum_{i_1=1}^{N_{pix,1}} p(\Omega_1(i_1)|x_1, \mathcal{H}^s) p(\Omega_1(i_1)|x_2, \mathcal{H}^s) \Delta A(i_1) \tag{5}$$

where $p(\Omega_1(i)|x_a, \mathcal{H}^s)$ is a probability density normalized so that $\sum_i p(\Omega_1(i)|x_a, \mathcal{H}^s)\Delta A = 1$. This algorithm can be extended to use a standard HEALPix secondary sky map by setting $p(\Omega_1(i_1)|x_2, \mathcal{H}^s) = P(\Omega_1(i_1)|x_2, \mathcal{H}^s)/\Delta A_2$ where $P(\Omega_1(i_1)|x_2, \mathcal{H}^s)$ is the probability in pixel i_1 and ΔA_2 is the pixel area of the second sky map. Another improvement that has been developed but still in the process of review is using the highest recursion depth of each MOC sky map using HP-MOC [64] and then going through the above algorithm, resulting in less error due to missing pixels of high probability density in the second sky map and slightly faster performance. In general, using MOC sky maps has a led to a 10-100x latency decrease in these operations and lower memory usage due to the smaller file size.

We expect the statistic in eqn (1) to generally have the properties of a FAR, assuming FAR_{gw} has these properties. Note that $R_{em}\Delta t$ is the expected number of random coincidences per GW candidate, which compensates for the reduction of joint candidates we expect to see by increasing their significance. In addition, we performed simulations that show that using uncorrelated sky maps gives $\langle \mathcal{I}_\Omega \rangle \approx 1$ in figures 3 and 5. Overall, this means we are convolving a FAR distribution with a random variable of mean 1, giving us a distribution that overall represents a FAR but could have skews in certain regions (see section IV).

B. Targeted GW-GRB Analysis

RAVEN is also used as an alert system for both the joint LVK-Fermi/GBM and LVK-*Swift* targeted searches. This involves the LVK sending moderately significant GW events to these experiments ($FAR < 2/day$), these external pipelines looking through their sub-threshold data for GRB counterparts, and sending this external candidate to us to process. RAVEN will then determine whether the joint event is publishable and then alert both LVK members and the external astronomical community of these events. The analysis used by RAVEN and these external experiments are meant to be identical, using the same search windows. Since this type of analysis is dominated by coincidences where both candidates are noise, we can write the joint ranking statistic Z as

$$Z = FAR_{gw} FAR_{ext} \Delta t \tag{6}$$

where FAR_{gw} and FAR_{ext} are the FARs of their respective experiments. This statistic can be mapped to a joint FAR since each individual FAR is drawn from a uniform distribution

$$FAR_t(Z) = \int_0^{Z_{max}} P(FAR_{ext}\Delta t \leq Z/FAR_{gw})\, dFAR_{gw} \tag{7}$$

$$= \int_0^{Z} dFAR_{gw} + \int_Z^{Z_{max}} Z/FAR_{gw}\, dFAR_{gw} \tag{8}$$

$$= Z\,(1 + \ln(Z_{max}/Z)) \tag{9}$$

where $Z_{max} = FAR_{gw,max} FAR_{ext,max} \Delta t$, given from the max FAR thresholds of each experiment. For instance, using the results from table II in the Fermi targeted search gives us $Z_{max} \approx 1.39 \times 10^{-8} Hz$, which looking at eqn (9) is also the max temporal joint FAR for this search. A final coincidence FAR_c with sky map information can be made by dividing by eqn (3) or eqn (5), similarly to eqn (1), to get

$$FAR_c = \frac{FAR_t}{\mathcal{I}_\Omega}. \tag{10}$$

It is worth noting the assumptions that go into these equations. According to [47, 48, 51] there are four possibilities if two events are truly unrelated, being that the individual events are any permutation of being real astrophysical signals or noise transients. In eqn (1) we assume the external triggers are significant and therefore the astrophysical rate will dominate, while we assume the GW candidates are not significant so the FAR dominates. In eqn (10) we assume both candidates are not significant, and therefore we use the FAR for each. If these assumptions break down, say in the case we have a significant binary black hole as one of the candidates, then it may be more appropriate to use that astrophysical rate instead of the GW FAR in the form of a later update notice. Using a combination of all these rates while resulting in a true joint FAR in the end is still an area of active research.

We note that sky maps from these external experiments may not provided in a timely manner or at all, so RAVEN will try to create an approximate Gaussian sky map for a external event based on the sky localization information from them, or simply calculate the joint FAR without this information if unavailable as well. We also recalculate the joint FAR whenever sky map information is updated, either from the external experiment or GW pipeline, in order to have the most up-to-date information in an alert. Next, for a coincidence to be published, the joint FAR (either eqn (1) or eqn (10) depending on the search) must be under predetermined thresholds.

C. GW-GRB Publishing Conditions

RAVEN is designed to be agnostic when searching for coincidences, but stringent when deciding to publish them. This is to alert LVK members internally of any potentially interesting candidates for further assessment, while avoiding sending too many false alarms to the external astronomical community. Regardless of whether a joint candidate passes the following publishing conditions for automatic alerts, the LVK Rapid Response Team have the ability to publish or retract candidates manually if the need arises.

RAVEN will automatically publish joint candidates that pass the following conditions:

1. The joint FAR, including trials factors, is lower than the public alert threshold (CBC: 1 per month, GW Burst: 1 per year.) The sky map overlap in eqn (3) must be included for all searches expected to have external sky maps. The only pipeline not currently providing this information is SNEWS.

2. The external candidate is not sub-threshold, i.e. considered significant apart from RAVEN. Subthreshold GRBs require further analysis and approval of experts from the corresponding external experiment before manually publishing.

3. The external candidate is not likely from an unrelated noise source, i.e. if classifications are available then there is at least a 50% probability the candidate is real.

4. An alert for the GW candidate has not been sent. RAVEN works with the current LVK alert system, adding additional information to the next alert if a coincidence is found. RAVEN is able to start this alert process if a joint candidate passes all publishing thresholds, but only if this hasn't been started already by the GW candidate itself.

The trials factors used here are worth expanding further upon. Since RAVEN both listens to multiple GW pipelines and is also calibrated to submit triggers at the rate of a GW pipeline to be included in the broader LVK alert system, the trials factor used is the product of these two effects. In other words if N is the number of independent GW pipelines (i.e. not counting RAVEN), the total trials factor is then $N(N+1)$. This product accounts for the number of GW pipelines used in the RAVEN analysis (N) and adjusts for the total number of pipelines publishing alerts, now includes RAVEN ($N+1$). This is a rather conservative estimate, approximately true at low significance, but at high significance, multiple GW searches tend to identify the same candidates and thus are not truly independent. The various GRB experiments have been combined by using the joint detected GRB rate as described in section III A.

D. GW Burst-SNEWS

Neutrino burst candidates from SNEWS have very low FARs ($< 1/100yr$) and also lack promptly available sky localizations [40], so the only determiner of their joint significance is the FARs of the GW candidates. We have chosen to publish joint GW Burst-SNEWS events if the GW candidate has a FAR of less than 1 per day after including the number of GW pipelines N as the trials factor. We also acknowledge the related low-latency GW-neutrino search, the Low-Latency Algorithm for Multi-messenger Astrophysics (LLAMA), designed specifically for this type of search [65, 66].

IV. SIMULATIONS

In order to test whether both eqn (1) and eqn (10) have the properties of a FAR, we created a background dataset by performing simulations of random coincidences. We simulated GW and Fermi/GBM-like GRB candidates with random event times during a period of 100 years, looking for events that fall within the given time window according to table I. We also repeated this analysis with *Swift*/BAT-like GRB candidates. Each simulation was run 50 times to measure the spread of results per inverse FAR bin. Each candidate's FAR was drawn from a uniform distribution, and the rates used are from table II.

We also wanted to understand the effect of sky maps in these simulations. We used sky maps from both sub-threshold GW candidates during O3 and real Fermi/GBM candidates [55, 67], indicative of both the targeted and untargeted search, respectively, and then compared this approach to using no sky map information (i.e. $\mathcal{I}_\Omega = 1$). For every coincidence, we drew a random sky map from each respective set, which effectively meant that the GRB and LVK sky maps were uncorrelated.

These results can be found in figures 2 and 4, where we see that both the untargeted and targeted methods generally result in sensible FARs without sky maps, while including this information causes the FAR to be underestimated due to a large number of low overlap joint events (see figures 3 and 5). This effect is even more pronounced for LVK-*Swift* events due to the general lower values of sky map overlap compared to LVK-Fermi and for the untargeted searches. This skew is inherent in the current method, as we have a uniform distribution (FAR) being convolved with another distribution (sky map overlap), which is not guaranteed to create another uniform distribution (joint FAR). In the case where we know what the two distributions will be beforehand, we can correct for skewness with an analytical transformation as in equation eqn (9) where we initially had two uniform distributions. However, the sky map overlap is dependent on the detectors and specifics of the individual candidate searches at the time and, therefore, has no obvious predetermined shape (see figures 3 and 5). The only trivial second distribution that results in a uniform distribution is that of unity, which we have done by setting $\mathcal{I}_\Omega = 1$ and labelled this as no sky map information in figures 2 and 4.

We could numerically correct for this skew after an operating run when all the candidates have been collected, similar to [48], by doing a simple remapping to the expected joint FAR. However, at the time of writing, there is no clear solution without knowing the sky map overlap distribution *a priori*. Even in the best case, using precomputed distributions presents a complex problem to avoid additional biases if changes to any of the searches are made midway through an operating run or, worse yet, the wrong assumptions are made.

Another approach we have tried is to construct p-value out of the sky map overlap and use a similar approach to III B to map back to a joint FAR. This has produced favourable results but suffers from the drawback that getting this p-value requires rotating and repeating the sky map overlap calculation many times to get a background distribution. Significantly increased latency and computational cost may not be worth it when initially trying to get an alert out, but could be viable at a later secondary refinement stage.

V. MOCK DATA CHALLENGE

Ahead of the fourth observing run (O4) of Advanced LIGO, Advanced Virgo, and KAGRA, several software and alert system enhancements were implemented since the conclusion of O3. To assess these upgrades, a Mock Data Challenge (MDC) was employed, designed to bolster the robustness of the low latency alert infrastructure system, as described in [28]. We also participated in this effort, both to have constant end-to-end testing of our system but also to get an idea of the latencies we can expect in the overall RAVEN pipeline.

We generated a joint candidate for every 10^{th} GW candidate, uploading 1 to 3 external events within the appropriate search window from table I. The multiple external events let us test how well our system handles high upload rates, as well as switching the preferred external event. This meant the injection rates much higher than in table II, which gave us ample testing coverage and assessment of latencies. For every external event we generated a sky map using a randomly sampled right ascension and declination, creating a Gaussian sky map with an appropriate standard deviation depending on the external pipeline used. We also sampled an external FAR if the external event was from a targeted search.

We found 469 joint candidates during this time, at which the time the temporal coincidence was discovered an `EM_COINC` label was assigned to the GW candidate. We can see the latencies of this label in figure 6. We found that only 356 of these joint candidates passed the publishing conditions described in III C, applying the `RAVEN_ALERT` label at that time. We can see the latencies of this label in figure 6. Note that `RAVEN_ALERT` itself will queue up an alert, which will take a variable amount of time based on whether a GW-only alert has already been triggered.

We can see the results of the latency analysis in figure 6. Considering that from [28] that superevents were created in 9.4s (50%) and 18.1s (90%), about one third of the latencies were waiting for the superevent to be created in the first place. This is latency that RAVEN cannot improve upon and is entirely dependent on the rest of the low-latency system to find GW candidates. Since we only injected external events once these GW candidates were uploaded (both creating the mock external event and then uploading it) this further added some latency that would may not be present in the production system. Real external candidates from an untargeted search would only be delayed by their own analysis, while events from the targeted search will have this inherent delay plus the typical intensive analysis of sub-threshold data.

Much of our heavier computational analysis occurs in the time between the `EM_COINC` and `RAVEN_ALERT` labels (joint FAR calculation, assessing publishing conditions, switching of preferred external event) which, looking at figure 6, typically only takes a few seconds to complete. This result is certainly within our design target. We should expect as improvements are made to the rest of the low-latency system that the latencies of `EM_COINC` and `RAVEN_ALERT` will decrease proportionally.

VI. DISCUSSION

We described the low-latency coincidence pipeline RAVEN, whose primary functions are to find interesting coincident astrophysical events and then to report these to the external astronomical community in a latency low enough to facilitate additional follow-up. We discussed the design of this pipeline, the methods to assign significance for both the targeted and untargeted searches, and ran simulations to measure their validity.

The choice to make RAVEN as agnostic as possible does come at the cost of sensitivity. For instance, we could choose to filter out likely binary black hole GW candidates by considering mass, effectively reducing our trials and increasing significance of the remaining candidates. We could also reduce our time windows in the wake of the 1.7 second delay between GW170817 and GRB 170817A, achieving a similar effect. However since there has been one confident GW-GRB detection, which has only begun to constrain coincidence models, we have decided to retain sensitivity to events that may be different than predicted by these models.

We also recognize the shortcomings of this method, especially with regards to the skewness in the joint FAR as discussed in section IV, but don't believe this invalidates the analysis. We must first recognize that this makes our method more conservative with regards to lower significance events, which is much more palatable compared to overestimating high significance events. This could lead to a loss of potentially interesting joint candidates, but will also definitely reduce the number of published false alarms as well. We emphasize that coincidences of any significance will be promptly reviewed manually by pipeline experts as they were in O3. Secondly, we must recall that the purpose of RAVEN is to rapidly alert astronomers, which already requires approximations for the sake of brevity. There exists more sophisticated methods of assigning significance with PyGRB and X-pipeline, but these operate with the goal being the more robust rather than computable in low latency [1]. Just like how GW pipelines use quick online template searches while at the same time more thorough offline searches exist, RAVEN lives in its niche as a rapid joint pipeline. We will keep exploring improvements to this method, including potentially using distance and inclination information, as well as using the sensitivity of the experiments to sky localization.

We also note that the joint FAR is likely not the best determiner of whether two events are truly coincident but instead whether the GW candidate should receive electromagnetic follow-up. For instance in the limit where the GW candidate is very significant, any association with an external event will likely pass the alert threshold while at the same time the sky map overlap integral may strongly argue against this being a real coincidence. Even in this case, the joint FAR is still useful for identifying events that warrant further follow-up (whether individually significant or already accompanied by another detection).

RAVEN will be an especially important tool in O4 and onward, potentially contributing to the number of BNS detections and maybe even helping to discover the first unmodeled GW transient.

---

[1] B. P. Abbott, R. Abbott, T. Abbott, M. Abernathy, F. Acernese, K. Ackley, C. Adams, T. Adams, P. Addesso, R. Adhikari, *et al.*, Search for gravitational waves associated with gamma-ray bursts during the first advanced ligo observing run and implications for the origin of grb 150906b, The Astrophysical Journal **841**, 89 (2017).

[2] B. P. Abbott, R. Abbott, T. Abbott, F. Acernese, K. Ackley, C. Adams, T. Adams, P. Addesso, R. Adhikari, V. Adya, *et al.*, Gravitational waves and gamma-rays from a binary neutron star merger: Gw170817 and grb 170817a, The Astrophysical Journal Letters **848**, L13 (2017).

[3] B. P. Abbott, R. Abbott, T. D. Abbott, S. Abraham, F. Acernese, K. Ackley, C. Adams, R. X. Adhikari, V. B. Adya, C. Affeldt, and et al., Search for gravitational-wave signals associated with gamma-ray bursts during the second observing run of advanced ligo and advanced virgo, The Astrophysical Journal **886**, 75 (2019).

[4] L.-V.-K. Collaboration and F. G.-R. B. M. Team, Gw170817 gcn circular, `https://gcn.gsfc.nasa.gov/other/G298048.gcn3` (2017), accessed: 2020-04-01.

[5] L.-V.-K. Collaboration, Gw170817 gracedb page, `https://gracedb.ligo.org/events/view/G298048` (2017), accessed: 2020-04-01.

[6] B. P. Abbott, R. Abbott, T. Abbott, F. Acernese, K. Ackley, C. Adams, T. Adams, P. Addesso, R. Adhikari, V. Adya, *et al.*, Gw170817: observation of gravitational waves from a binary neutron star inspiral, Physical Review Letters **119**, 161101 (2017).

[7] A. Goldstein, P. Veres, E. Burns, M. Briggs, R. Hamburg, D. Kocevski, C. Wilson-Hodge, R. Preece, S. Poolakkil,

O. Roberts, *et al.*, An ordinary short gamma-ray burst with extraordinary implications: Fermi-gbm detection of grb 170817a, The Astrophysical Journal Letters **848**, L14 (2017).

[8] B. P. Abbott, R. Abbott, T. D. Abbott, F. Acernese, K. Ackley, C. Adams, T. Adams, P. Addesso, R. X. Adhikari, V. B. Adya, C. Affeldt, M. Afrough, B. Agarwal, M. Agathos, K. Agatsuma, N. Aggarwal, O. D. Aguiar, L. Aiello, A. Ain, P. Ajith, B. Allen, G. Allen, A. Allocca, P. A. Altin, A. Amato, A. Ananyeva, S. B. Anderson, W. G. Anderson, S. V. Angelova, S. Antier, S. Appert, K. Arai, M. C. Araya, J. S. Areeda, N. Arnaud, K. G. Arun, S. Ascenzi, G. Ashton, M. Ast, S. M. Aston, P. Astone, D. V. Atallah, P. Aufmuth, C. Aulbert, K. AultONeal, C. Austin, A. Avila-Alvarez, S. Babak, P. Bacon, M. K. M. Bader, S. Bae, P. T. Baker, F. Baldaccini, G. Ballardin, S. W. Ballmer, S. Banagiri, J. C. Barayoga, S. E. Barclay, B. C. Barish, D. Barker, K. Barkett, F. Barone, B. Barr, L. Barsotti, M. Barsuglia, D. Barta, S. D. Barthelmy, J. Bartlett, I. Bartos, R. Bassiri, A. Basti, J. C. Batch, M. Bawaj, J. C. Bayley, M. Bazzan, B. Bécsy, C. Beer, M. Bejger, I. Belahcene, A. S. Bell, B. K. Berger, G. Bergmann, J. J. Bero, C. P. L. Berry, D. Bersanetti, A. Bertolini, J. Betzwieser, S. Bhagwat, R. Bhandare, I. A. Bilenko, G. Billingsley, C. R. Billman, J. Birch, R. Birney, O. Birnholtz, S. Biscans, S. Biscoveanu, A. Bisht, M. Bitossi, C. Biwer, M. A. Bizouard, J. K. Blackburn, J. Blackman, C. D. Blair, D. G. Blair, R. M. Blair, S. Bloemen, O. Bock, N. Bode, M. Boer, G. Bogaert, A. Bohe, F. Bondu, E. Bonilla, R. Bonnand, B. A. Boom, R. Bork, V. Boschi, S. Bose, K. Bossie, Y. Bouffanais, A. Bozzi, C. Bradaschia, P. R. Brady, M. Branchesi, J. E. Brau, T. Briant, A. Brillet, M. Brinkmann, V. Brisson, P. Brockill, J. E. Broida, A. F. Brooks, D. A. Brown, D. D. Brown, S. Brunett, C. C. Buchanan, A. Buikema, T. Bulik, H. J. Bulten, A. Buonanno, D. Buskulic, C. Buy, R. L. Byer, M. Cabero, L. Cadonati, G. Cagnoli, C. Cahillane, J. Calderón Bustillo, T. A. Callister, E. Calloni, J. B. Camp, M. Canepa, P. Canizares, K. C. Cannon, H. Cao, J. Cao, C. D. Capano, E. Capocasa, F. Carbognani, S. Caride, M. F. Carney, J. Casanueva Diaz, C. Casentini, S. Caudill, M. Cavaglià, F. Cavalier, R. Cavalieri, G. Cella, C. B. Cepeda, P. Cerdá-Durán, G. Cerretani, E. Cesarini, S. J. Chamberlin, M. Chan, S. Chao, P. Charlton, E. Chase, E. Chassande-Mottin, D. Chatterjee, K. Chatziioannou, B. D. Cheeseboro, H. Y. Chen, X. Chen, Y. Chen, H. P. Cheng, H. Chia, A. Chincarini, A. Chiummo, T. Chmiel, H. S. Cho, M. Cho, J. H. Chow, N. Christensen, Q. Chu, A. J. K. Chua, S. Chua, A. K. W. Chung, S. Chung, and G. Ciani, Multi-messenger Observations of a Binary Neutron Star Merger, ApJ Lett. **848**, L12 (2017), arXiv:1710.05833 [astro-ph.HE].

[9] LIGO Scientific Collaboration, J. Aasi, B. P. Abbott, R. Abbott, T. Abbott, M. R. Abernathy, K. Ackley, C. Adams, T. Adams, P. Addesso, R. X. Adhikari, V. Adya, C. Affeldt, N. Aggarwal, O. D. Aguiar, A. Ain, P. Ajith, A. Alemic, B. Allen, D. Amariutei, S. B. Anderson, W. G. Anderson, K. Arai, M. C. Araya, C. Arceneaux, J. S. Areeda, G. Ashton, S. Ast, S. M. Aston, P. Aufmuth, C. Aulbert, B. E. Aylott, S. Babak, P. T. Baker, S. W. Ballmer, J. C. Barayoga, M. Barbet, S. Barclay, B. C. Barish, D. Barker, B. Barr, L. Barsotti, J. Bartlett, M. A. Barton, I. Bartos, R. Bassiri, J. C. Batch, C. Baune, B. Behnke, A. S. Bell, C. Bell, M. Benacquista, J. Bergman, G. Bergmann, C. P. L. Berry, J. Betzwieser, S. Bhagwat, R. Bhandare, I. A. Bilenko, G. Billingsley, J. Birch, S. Biscans, C. Biwer, J. K. Blackburn, L. Blackburn, C. D. Blair, D. Blair, O. Bock, T. P. Bodiya, P. Bojtos, C. Bond, R. Bork, M. Born, S. Bose, P. R. Brady, V. B. Braginsky, J. E. Brau, D. O. Bridges, M. Brinkmann, A. F. Brooks, D. A. Brown, D. D. Brown, N. M. Brown, S. Buchman, A. Buikema, A. Buonanno, L. Cadonati, J. Calderón Bustillo, J. B. Camp, K. C. Cannon, J. Cao, C. D. Capano, S. Caride, S. Caudill, M. Cavaglià, C. Cepeda, R. Chakraborty, T. Chalermsongsak, S. J. Chamberlin, S. Chao, P. Charlton, Y. Chen, H. S. Cho, M. Cho, J. H. Chow, N. Christensen, Q. Chu, S. Chung, G. Ciani, F. Clara, J. A. Clark, C. Collette, L. Cominsky, M. Constancio, Jr., D. Cook, T. R. Corbitt, N. Cornish, A. Corsi, C. A. Costa, M. W. Coughlin, S. Countryman, P. Couvares, D. M. Coward, M. J. Cowart, D. C. Coyne, R. Coyne, K. Craig, J. D. E. Creighton, T. D. Creighton, J. Cripe, S. G. Crowder, A. Cumming, L. Cunningham, C. Cutler, K. Dahl, T. Dal Canton, M. Damjanic, S. L. Danilishin, K. Danzmann, L. Dartez, I. Dave, H. Daveloza, G. S. Davies, E. J. Daw, D. DeBra, W. Del Pozzo, T. Denker, T. Dent, V. Dergachev, R. T. DeRosa, R. DeSalvo, S. Dhurandhar, M. D´ıaz, I. Di Palma, G. Dojcinoski, E. Dominguez, F. Donovan, K. L. Dooley, S. Doravari, R. Douglas, T. P. Downes, J. C. Driggers, Z. Du, S. Dwyer, T. Eberle, T. Edo, M. Edwards, M. Edwards, A. Effler, H. B. Eggenstein, P. Ehrens, J. Eichholz, S. S. Eikenberry, R. Essick, T. Etzel, M. Evans, T. Evans, M. Factourovich, S. Fairhurst, X. Fan, Q. Fang, B. Farr, W. M. Farr, M. Favata, M. Fays, H. Fehrmann, M. M. Fejer, D. Feldbaum, E. C. Ferreira, R. P. Fisher, Z. Frei, A. Freise, R. Frey, T. T. Fricke, P. Fritschel, V. V. Frolov, S. Fuentes-Tapia, P. Fulda, M. Fyffe, and J. R. Gair, Advanced LIGO, Classical and Quantum Gravity **32**, 074001 (2015), arXiv:1411.4547 [gr-qc].

[10] F. Acernese, M. Agathos, K. Agatsuma, D. Aisa, N. Allemandou, A. Allocca, J. Amarni, P. Astone, G. Balestri, G. Ballardin, F. Barone, J. P. Baronick, M. Barsuglia, A. Basti, F. Basti, T. S. Bauer, V. Bavigadda, M. Bejger, M. G. Beker, C. Belczynski, D. Bersanetti, A. Bertolini, M. Bitossi, M. A. Bizouard, S. Bloemen, M. Blom, M. Boer, G. Bogaert, D. Bondi, F. Bondu, L. Bonelli, R. Bonnand, V. Boschi, L. Bosi, T. Bouedo, C. Bradaschia, M. Branchesi, T. Briant, A. Brillet, V. Brisson, T. Bulik, H. J. Bulten, D. Buskulic, C. Buy, G. Cagnoli, E. Calloni, C. Campeggi, B. Canuel, F. Carbognani, F. Cavalier, R. Cavalieri, G. Cella, E. Cesarini, E. C. Mottin, A. Chincarini, A. Chiummo, S. Chua, F. Cleva, E. Coccia, P. F. Cohadon, A. Colla, M. Colombini, A. Conte, J. P. Coulon, E. Cuoco, A. Dalmaz, S. D'Antonio, V. Dattilo, M. Davier, R. Day, G. Debreczeni, J. Degallaix, S. Deléglise, W. D. Pozzo, H. Dereli, R. D. Rosa, L. D. Fiore, A. D. Lieto, A. D. Virgilio, M. Doets, V. Dolique, M. Drago, M. Ducrot, G. Endrőczi, V. Fafone, S. Farinon, I. Ferrante, F. Ferrini, F. Fidecaro, I. Fiori, R. Flaminio, J. D. Fournier, S. Franco, S. Frasca, F. Frasconi, L. Gammaitoni, F. Garufi, M. Gaspard, A. Gatto, G. Gemme, B. Gendre, E. Genin, A. Gennai, S. Ghosh, L. Giacobone, A. Giazotto, R. Gouaty, M. Granata, G. Greco, P. Groot, G. M. Guidi, J. Harms, A. Heidmann, H. Heitmann, P. Hello,

G. Hemming, E. Hennes, D. Hofman, P. Jaranowski, R. J. G. Jonker, M. Kasprzack, F. Kéfélian, I. Kowalska, M. Kraan, A. Królak, A. Kutynia, C. Lazzaro, M. Leonardi, N. Leroy, N. Letendre, T. G. F. Li, B. Lieunard, M. Lorenzini, V. Loriette, G. Losurdo, C. Magazzù, E. Majorana, I. Maksimovic, V. Malvezzi, N. Man, V. Mangano, M. Mantovani, F. Marchesoni, F. Marion, J. Marque, F. Martelli, L. Martellini, A. Masserot, D. Meacher, J. Meidam, F. Mezzani, C. Michel, L. Milano, Y. Minenkov, A. Moggi, M. Mohan, M. Montani, N. Morgado, B. Mours, F. Mul, M. F. Nagy, I. Nardecchia, L. Naticchioni, G. Nelemans, I. Neri, M. Neri, F. Nocera, E. Pacaud, C. Palomba, F. Paoletti, A. Paoli, A. Pasqualetti, R. Passaquieti, D. Passuello, M. Perciballi, S. Petit, M. Pichot, F. Piergiovanni, G. Pillant, A. Piluso, L. Pinard, R. Poggiani, M. Prijatelj, G. A. Prodi, M. Punturo, P. Puppo, D. S. Rabeling, I. Rácz, P. Rapagnani, M. Razzano, V. Re, T. Regimbau, F. Ricci, F. Robinet, A. Rocchi, L. Rolland, R. Romano, D. Rosińska, P. Ruggi, and E. Saracco, Advanced Virgo: a second-generation interferometric gravitational wave detector, Classical and Quantum Gravity **32**, 024001 (2015), arXiv:1408.3978 [gr-qc].

[11] T. Akutsu, M. Ando, K. Arai, Y. Arai, S. Araki, A. Araya, N. Aritomi, Y. Aso, S. Bae, Y. Bae, L. Baiotti, R. Bajpai, M. A. Barton, K. Cannon, E. Capocasa, M. Chan, C. Chen, K. Chen, Y. Chen, H. Chu, Y. K. Chu, S. Eguchi, Y. Enomoto, R. Flaminio, Y. Fujii, M. Fukunaga, M. Fukushima, G. Ge, A. Hagiwara, S. Haino, K. Hasegawa, H. Hayakawa, K. Hayama, Y. Himemoto, Y. Hiranuma, N. Hirata, E. Hirose, Z. Hong, B. H. Hsieh, C. Z. Huang, P. Huang, Y. Huang, B. Ikenoue, S. Imam, K. Inayoshi, Y. Inoue, K. Ioka, Y. Itoh, K. Izumi, K. Jung, P. Jung, T. Kajita, M. Kamiizumi, N. Kanda, G. Kang, K. Kawaguchi, N. Kawai, T. Kawasaki, C. Kim, J. C. Kim, W. S. Kim, Y. M. Kim, N. Kimura, N. Kita, H. Kitazawa, Y. Kojima, K. Kokeyama, K. Komori, A. K. H. Kong, K. Kotake, C. Kozakai, R. Kozu, R. Kumar, J. Kume, C. Kuo, H. S. Kuo, S. Kuroyanagi, K. Kusayanagi, K. Kwak, H. K. Lee, H. W. Lee, R. Lee, M. Leonardi, L. C. C. Lin, C. Y. Lin, F. L. Lin, G. C. Liu, L. W. Luo, M. Marchio, Y. Michimura, N. Mio, O. Miyakawa, A. Miyamoto, Y. Miyazaki, K. Miyo, S. Miyoki, S. Morisaki, Y. Moriwaki, K. Nagano, S. Nagano, K. Nakamura, H. Nakano, M. Nakano, R. Nakashima, T. Narikawa, R. Negishi, W. T. Ni, A. Nishizawa, Y. Obuchi, W. Ogaki, J. J. Oh, S. H. Oh, M. Ohashi, N. Ohishi, M. Ohkawa, K. Okutomi, K. Oohara, C. P. Ooi, S. Oshino, K. Pan, H. Pang, J. Park, F. E. P. Arellano, I. Pinto, N. Sago, S. Saito, Y. Saito, K. Sakai, Y. Sakai, Y. Sakuno, S. Sato, T. Sato, T. Sawada, T. Sekiguchi, Y. Sekiguchi, S. Shibagaki, R. Shimizu, T. Shimoda, K. Shimode, H. Shinkai, T. Shishido, A. Shoda, K. Somiya, E. J. Son, H. Sotani, R. Sugimoto, T. Suzuki, T. Suzuki, H. Tagoshi, H. Takahashi, R. Takahashi, A. Takamori, S. Takano, H. Takeda, M. Takeda, H. Tanaka, K. Tanaka, K. Tanaka, T. Tanaka, T. Tanaka, S. Tanioka, E. N. Tapia San Martin, S. Telada, T. Tomaru, Y. Tomigami, T. Tomura, F. Travasso, L. Trozzo, T. Tsang, K. Tsubono, S. Tsuchida, T. Tsuzuki, D. Tuyenbayev, N. Uchikata, T. Uchiyama, A. Ueda, T. Uehara, K. Ueno, G. Ueshima, F. Uraguchi, T. Ushiba, M. H. P. M. van Putten, H. Vocca, J. Wang, C. Wu, H. Wu, S. Wu, W. R. Xu, T. Yamada, K. Yamamoto, K. Yamamoto, T. Yamamoto, K. Yokogawa, J. Yokoyama, T. Yokozawa, T. Yoshioka, H. Yuzurihara, S. Zeidler, Y. Zhao, and Z. H. Zhu, Overview of KAGRA: Detector design and construction history, Progress of Theoretical and Experimental Physics **2021**, 05A101 (2021), arXiv:2005.05574 [physics.ins-det].

[12] B. P. Abbott, R. Abbott, T. D. Abbott, M. R. Abernathy, F. Acernese, K. Ackley, C. Adams, T. Adams, P. Addesso, R. X. Adhikari, V. B. Adya, C. Affeldt, M. Agathos, K. Agatsuma, N. Aggarwal, O. D. Aguiar, L. Aiello, A. Ain, P. Ajith, T. Akutsu, B. Allen, A. Allocca, P. A. Altin, A. Ananyeva, S. B. Anderson, W. G. Anderson, M. Ando, S. Appert, K. Arai, A. Araya, M. C. Araya, J. S. Areeda, N. Arnaud, K. G. Arun, H. Asada, S. Ascenzi, G. Ashton, Y. Aso, M. Ast, S. M. Aston, P. Astone, S. Atsuta, P. Aufmuth, C. Aulbert, A. Avila-Alvarez, K. Awai, S. Babak, P. Bacon, M. K. M. Bader, L. Baiotti, P. T. Baker, F. Baldaccini, G. Ballardin, S. W. Ballmer, J. C. Barayoga, S. E. Barclay, B. C. Barish, D. Barker, F. Barone, B. Barr, L. Barsotti, M. Barsuglia, D. Barta, J. Bartlett, M. A. Barton, I. Bartos, R. Bassiri, A. Basti, J. C. Batch, C. Baune, V. Bavigadda, M. Bazzan, B. Bécsy, C. Beer, M. Bejger, I. Belahcene, M. Belgin, A. S. Bell, B. K. Berger, G. Bergmann, C. P. L. Berry, D. Bersanetti, A. Bertolini, J. Betzwieser, S. Bhagwat, R. Bhandare, I. A. Bilenko, G. Billingsley, C. R. Billman, J. Birch, R. Birney, O. Birnholtz, S. Biscans, A. Bisht, M. Bitossi, C. Biwer, M. A. Bizouard, J. K. Blackburn, J. Blackman, C. D. Blair, D. G. Blair, R. M. Blair, S. Bloemen, O. Bock, M. Boer, G. Bogaert, A. Bohe, F. Bondu, R. Bonnand, B. A. Boom, R. Bork, V. Boschi, S. Bose, Y. Bouffanais, A. Bozzi, C. Bradaschia, P. R. Brady, V. B. Braginsky, M. Branchesi, J. E. Brau, T. Briant, A. Brillet, M. Brinkmann, V. Brisson, P. Brockill, J. E. Broida, A. F. Brooks, D. A. Brown, D. D. Brown, N. M. Brown, S. Brunett, C. C. Buchanan, A. Buikema, T. Bulik, H. J. Bulten, A. Buonanno, D. Buskulic, C. Buy, R. L. Byer, M. Cabero, L. Cadonati, G. Cagnoli, C. Cahillane, J. Calderón Bustillo, T. A. Callister, E. Calloni, J. B. Camp, K. C. Cannon, H. Cao, J. Cao, C. D. Capano, E. Capocasa, F. Carbognani, S. Caride, J. Casanueva Diaz, C. Casentini, S. Caudill, M. Cavaglià, F. Cavalier, R. Cavalieri, G. Cella, C. B. Cepeda, L. Cerboni Baiardi, G. Cerretani, E. Cesarini, S. J. Chamberlin, M. Chan, S. Chao, P. Charlton, E. Chassande-Mottin, B. D. Cheeseboro, H. Y. Chen, Y. Chen, H. P. Cheng, A. Chincarini, A. Chiummo, T. Chmiel, H. S. Cho, M. Cho, J. H. Chow, N. Christensen, Q. Chu, A. J. K. Chua, S. Chua, S. Chung, G. Ciani, F. Clara, J. A. Clark, F. Cleva, C. Cocchieri, E. Coccia, P. F. Cohadon, A. Colla, C. G. Collette, L. Cominsky, M. Constancio, L. Conti, S. J. Cooper, T. R. Corbitt, and N. Cornish, Prospects for observing and localizing gravitational-wave transients with Advanced LIGO, Advanced Virgo and KAGRA, Living Reviews in Relativity **21**, 3 (2018), arXiv:1304.0670 [gr-qc].

[13] `https://gracedb.ligo.org/events/view/G298048`.

[14] V. Connaughton, GBM-LIGO Group, L. Blackburn, M. S. Briggs, J. Broida, E. Burns, J. Camp, T. Dal Canton, N. Christensen, A. Goldstein, R. Hamburg, C. M. Hui, P. Jenke, D. Kocevski, N. Leroy, T. Littenberg, J. McEnery, R. Preece, J. Racusin, P. Shawhan,

K. Siellez, L. Singer, J. Veitch, P. Veres, and C. Wilson-Hodge, LIGO/Virgo G298048: Fermi GBM trigger 170817.529 and LIGO single IFO trigger, GRB Coordinates Network **21506**, 1 (2017).

[15] LIGO Scientific Collaboration and Virgo Collaboration, LIGO/Virgo G298048: Fermi GBM trigger 524666471/170817529: LIGO/Virgo Identification of a possible gravitational-wave counterpart, GRB Coordinates Network **21505**, 1 (2017).

[16] S. Valenti, J. David, S. Yang, E. Cappellaro, L. Tartaglia, A. Corsi, S. W. Jha, D. E. Reichart, J. Haislip, and V. Kouprianov, The discovery of the electromagnetic counterpart of gw170817: kilonova at 2017gfo/dlt17ck, The Astrophysical Journal Letters **848**, L24 (2017).

[17] D. A. Coulter, R. J. Foley, C. D. Kilpatrick, M. R. Drout, A. L. Piro, B. J. Shappee, M. R. Siebert, J. D. Simon, N. Ulloa, D. Kasen, B. F. Madore, A. Murguia-Berthier, Y. C. Pan, J. X. Prochaska, E. Ramirez-Ruiz, A. Rest, and C. Rojas-Bravo, Swope Supernova Survey 2017a (SSS17a), the optical counterpart to a gravitational wave source, Science **358**, 1556 (2017), arXiv:1710.05452 [astro-ph.HE].

[18] R. Hamburg, C. Fletcher, E. Burns, A. Goldstein, E. Bissaldi, M. S. Briggs, W. H. Cleveland, M. M. Giles, C. M. Hui, D. Kocevski, S. Lesage, B. Mailyan, C. Malacaria, S. Poolakkil, R. Preece, O. J. Roberts, P. Veres, A. von Kienlin, C. A. Wilson-Hodge, J. Wood, Fermi Gamma-Ray Burst Monitor, R. Abbott, T. D. Abbott, S. Abraham, F. Acernese, K. Ackley, C. Adams, R. X. Adhikari, V. B. Adya, C. Affeldt, M. Agathos, K. Agatsuma, N. Aggarwal, O. D. Aguiar, A. Aich, L. Aiello, A. Ain, P. Ajith, G. Allen, A. Allocca, P. A. Altin, A. Amato, S. Anand, A. Ananyeva, S. B. Anderson, W. G. Anderson, S. V. Angelova, S. Ansoldi, S. Antier, S. Appert, K. Arai, M. C. Araya, J. S. Areeda, M. Arène, N. Arnaud, S. M. Aronson, S. Ascenzi, G. Ashton, S. M. Aston, P. Astone, F. Aubin, P. Aufmuth, K. AultONeal, C. Austin, V. Avendano, S. Babak, P. Bacon, F. Badaracco, M. K. M. Bader, S. Bae, A. M. Baer, J. Baird, F. Baldaccini, G. Ballardin, S. W. Ballmer, A. Bals, A. Balsamo, G. Baltus, S. Banagiri, D. Bankar, R. S. Bankar, J. C. Barayoga, C. Barbieri, B. C. Barish, D. Barker, K. Barkett, P. Barneo, F. Barone, B. Barr, L. Barsotti, M. Barsuglia, D. Barta, J. Bartlett, I. Bartos, R. Bassiri, A. Basti, M. Bawaj, J. C. Bayley, M. Bazzan, B. Bécsy, M. Bejger, I. Belahcene, A. S. Bell, D. Beniwal, M. G. Benjamin, J. D. Bentley, F. Bergamin, B. K. Berger, G. Bergmann, S. Bernuzzi, C. P. L. Berry, D. Bersanetti, A. Bertolini, J. Betzwieser, R. Bhandare, A. V. Bhandari, J. Bidler, E. Biggs, I. A. Bilenko, G. Billingsley, R. Birney, O. Birnholtz, S. Biscans, M. Bischi, S. Biscoveanu, A. Bisht, G. Bissenbayeva, M. Bitossi, M. A. Bizouard, J. K. Blackburn, J. Blackman, C. D. Blair, D. G. Blair, R. M. Blair, F. Bobba, N. Bode, M. Boer, Y. Boetzel, G. Bogaert, F. Bondu, E. Bonilla, R. Bonnand, P. Booker, B. A. Boom, R. Bork, V. Boschi, S. Bose, V. Bossilkov, J. Bosveld, Y. Bouffanais, A. Bozzi, C. Bradaschia, P. R. Brady, A. Bramley, M. Branchesi, J. E. Brau, M. Breschi, T. Briant, J. H. Briggs, F. Brighenti, A. Brillet, M. Brinkmann, P. Brockill, A. F. Brooks, J. Brooks, D. D. Brown, S. Brunett, G. Bruno, R. Bruntz, A. Buikema, T. Bulik, H. J. Bulten, A. Buonanno, D. Buskulic, R. L. Byer, M. Cabero, L. Cadonati, G. Cagnoli, C. Cahillane, J. Calderón Bustillo, J. D. Callaghan, T. A. Callister, E. Calloni, J. B. Camp, M. Canepa, K. C. Cannon, H. Cao, J. Cao, G. Carapella, F. Carbognani, S. Caride, M. F. Carney, G. Carullo, J. Casanueva Diaz, C. Casentini, J. Castañeda, S. Caudill, M. Cavaglià, F. Cavalier, and R. Cavalieri, A Joint Fermi-GBM and LIGO/Virgo Analysis of Compact Binary Mergers from the First and Second Gravitational-wave Observing Runs, Astrophys. J. **893**, 100 (2020), arXiv:2001.00923 [astro-ph.HE].

[19] C. Fletcher, J. Wood, R. Hamburg, P. Veres, C. M. Hui, E. Bissaldi, M. S. Briggs, E. Burns, W. H. Cleveland, M. M. Giles, A. Goldstein, B. A. Hristov, D. Kocevski, S. Lesage, B. Mailyan, C. Malacaria, S. Poolakkil, A. von Kienlin, C. A. Wilson-Hodge, Fermi Gamma-Ray Burst Monitor Team, M. Crnogorčević, J. Delaunay, A. Tohuvavohu, R. Caputo, S. B. Cenko, S. Laha, T. Parsotan, R. Abbott, H. Abe, F. Acernese, K. Ackley, N. Adhikari, R. X. Adhikari, V. K. Adkins, V. B. Adya, C. Affeldt, D. Agarwal, M. Agathos, K. Agatsuma, N. Aggarwal, O. D. Aguiar, L. Aiello, A. Ain, P. Ajith, T. Akutsu, S. Albanesi, R. A. Alfaidi, A. Allocca, P. A. Altin, A. Amato, C. Anand, S. Anand, A. Ananyeva, S. B. Anderson, W. G. Anderson, M. Ando, T. Andrade, N. Andres, M. Andrés-Carcasona, T. Andrić, S. V. Angelova, S. Ansoldi, J. M. Antelis, S. Antier, T. Apostolatos, E. Z. Appavuravther, S. Appert, S. K. Apple, K. Arai, A. Araya, M. C. Araya, J. S. Areeda, M. Arène, N. Aritomi, N. Arnaud, M. Arogeti, S. M. Aronson, K. G. Arun, H. Asada, Y. Asali, G. Ashton, Y. Aso, M. Assiduo, S. Assis de Souza Melo, S. M. Aston, P. Astone, F. Aubin, K. Aultoneal, C. Austin, S. Babak, F. Badaracco, M. K. M. Bader, C. Badger, S. Bae, Y. Bae, A. M. Baer, S. Bagnasco, Y. Bai, J. Baird, R. Bajpai, T. Baka, M. Ball, G. Ballardin, S. W. Ballmer, A. Balsamo, G. Baltus, S. Banagiri, B. Banerjee, D. Bankar, J. C. Barayoga, C. Barbieri, B. C. Barish, D. Barker, P. Barneo, F. Barone, B. Barr, L. Barsotti, M. Barsuglia, D. Barta, J. Bartlett, M. A. Barton, I. Bartos, S. Basak, R. Bassiri, A. Basti, M. Bawaj, J. C. Bayley, M. Bazzan, B. R. Becher, B. Bécsy, V. M. Bedakihale, F. Beirnaert, M. Bejger, I. Belahcene, V. Benedetto, D. Beniwal, M. G. Benjamin, T. F. Bennett, J. D. Bentley, M. Benyaala, S. Bera, M. Berbel, F. Bergamin, B. K. Berger, S. Bernuzzi, C. P. L. Berry, D. Bersanetti, A. Bertolini, J. Betzwieser, D. Beveridge, R. Bhandare, A. V. Bhandari, U. Bhardwaj, R. Bhatt, D. Bhattacharjee, S. Bhaumik, A. Bianchi, I. A. Bilenko, G. Billingsley, S. Bini, R. Birney, O. Birnholtz, S. Biscans, M. Bischi, S. Biscoveanu, A. Bisht, B. Biswas, M. Bitossi, M. A. Bizouard, J. K. Blackburn, C. D. Blair, D. G. Blair, R. M. Blair, F. Bobba, N. Bode, M. Boër, G. Bogaert, M. Boldrini, G. N. Bolingbroke, L. D. Bonavena, F. Bondu, E. Bonilla, R. Bonnand, P. Booker, B. A. Boom, R. Bork, V. Boschi, N. Bose, S. Bose, V. Bossilkov, V. Boudart, Y. Bouffanais, A. Bozzi, C. Bradaschia, P. R. Brady, A. Bramley, A. Branch, M. Branchesi, J. E. Brau, and M. Breschi, A Joint Fermi-GBM and Swift-BAT Analysis of Gravitational-wave Candidates from the Third Gravitational-wave Observing Run, Astrophys. J. **964**, 149 (2024), arXiv:2308.13666 [astro-ph.HE].

[20] G. Raman, S. Ronchini, J. Delaunay, A. Tohuvavohu, J. A. Kennea, T. Parsotan, E. Ambrosi, M. Grazia Bernardini, S. Campana, G. Cusumano, A. D'Ai,

P. D'Avanzo, V. D'Elia, M. De Pasquale, S. Dichiara, P. Evans, D. Hartmann, P. Kuin, A. Melandri, P. O'Brien, J. P. Osborne, K. Page, D. M. Palmer, B. Sbarufatti, G. Tagliaferri, E. Troja, A. G. Abac, R. Abbott, H. Abe, I. Abouelfettouh, F. Acernese, K. Ackley, C. Adamcewicz, S. Adhicary, N. Adhikari, R. X. Adhikari, V. K. Adkins, V. B. Adya, C. Affeldt, D. Agarwal, M. Agathos, O. D. Aguiar, I. Aguilar, L. Aiello, A. Ain, T. Akutsu, S. Albanesi, R. A. Alfaidi, A. Al-Jodah, C. Alléné, A. Allocca, S. Al-Shammari, P. A. Altin, S. Alvarez-Lopez, A. Amato, L. Amez-Droz, A. Amorosi, C. Amra, S. Anand, A. Ananyeva, S. B. Anderson, W. G. Anderson, M. Andia, M. Ando, T. Andrade, N. Andres, M. Andrés-Carcasona, T. Andrić, J. Anglin, S. Ansoldi, J. M. Antelis, S. Antier, M. Aoumi, E. Z. Appavuravther, S. Appert, S. K. Apple, K. Arai, A. Araya, M. C. Araya, J. S. Areeda, N. Aritomi, F. Armato, N. Arnaud, M. Arogeti, S. M. Aronson, G. Ashton, Y. Aso, M. Assiduo, S. Assis de Souza Melo, S. M. Aston, P. Astone, F. Aubin, K. AultONeal, G. Avallone, S. Babak, F. Badaracco, C. Badger, S. Bae, S. Bagnasco, E. Bagui, Y. Bai, J. G. Baier, R. Bajpai, T. Baka, M. Ball, G. Ballardin, S. W. Ballmer, S. Banagiri, B. Banerjee, D. Bankar, P. Baral, J. C. Barayoga, B. C. Barish, D. Barker, P. Barneo, F. Barone, B. Barr, L. Barsotti, M. Barsuglia, D. Barta, S. D. Barthelmy, M. A. Barton, I. Bartos, S. Basak, A. Basalaev, R. Bassiri, A. Basti, M. Bawaj, P. Baxi, J. C. Bayley, A. C. Baylor, M. Bazzan, B. Bécsy, V. M. Bedakihale, F. Beirnaert, M. Bejger, D. Belardinelli, A. S. Bell, V. Benedetto, D. Beniwal, W. Benoit, J. D. Bentley, M. Ben Yaala, S. Bera, M. Berbel, F. Bergamin, B. K. Berger, S. Bernuzzi, M. Beroiz, C. P. L. Berry, D. Bersanetti, A. Bertolini, J. Betzwieser, D. Beveridge, N. Bevins, R. Bhandare, U. Bhardwaj, R. Bhatt, D. Bhattacharjee, S. Bhaumik, S. Bhowmick, A. Bianchi, I. A. Bilenko, G. Billingsley, A. Binetti, S. Bini, O. Birnholtz, S. Biscoveanu, A. Bisht, M. Bitossi, M. A. Bizouard, J. K. Blackburn, C. D. Blair, D. G. Blair, F. Bobba, N. Bode, G. Bogaert, G. Boileau, M. Boldrini, G. N. Bolingbroke, A. Bolliand, L. D. Bonavena, R. Bondarescu, F. Bondu, E. Bonilla, M. S. Bonilla, A. Bonino, R. Bonnand, P. Booker, A. Borchers, V. Boschi, S. Bose, V. Bossilkov, V. Boudart, A. Boumerdassi, A. Bozzi, C. Bradaschia, P. R. Brady, M. Braglia, and A. Branch, Swift-BAT GUANO follow-up of gravitational-wave triggers in the third LIGO-Virgo-KAGRA observing run, arXiv e-prints , arXiv:2407.12867 (2024), arXiv:2407.12867 [astro-ph.HE].

[21] A. Ursi, F. Verrecchia, G. Piano, C. Casentini, M. Tavani, A. Bulgarelli, M. Cardillo, F. Longo, F. Lucarelli, A. Morselli, N. Parmiggiani, M. Pilia, C. Pittori, and A. Rappoldi, AGILE Observations of the LIGO-Virgo Gravitational-wave Events of the GWTC-1 Catalog, Astrophys. J. **924**, 80 (2022).

[22] A. Ridnaia, D. Svinkin, and D. Frederiks, A search for gamma-ray counterparts to gravitational wave events in Konus-Wind data, in *Journal of Physics Conference Series*, Journal of Physics Conference Series, Vol. 1697 (IOP, 2020) p. 012030.

[23] G. Waratkar, V. Bhalerao, and D. Bhattacharya, Bright in the Black: Searching for Electromagnetic Counterparts to Gravitational-wave Candidates in LIGO-Virgo-KAGRA Observation Runs with AstroSat-CZTI, Astrophys. J. **976**, 123 (2024), arXiv:2402.07564 [astro-ph.HE].

[24] R. A. Street, M. Bowman, E. S. Saunders, and T. Boroson, General-purpose software for managing astronomical observing programs in the LSST era, in *Software and Cyberinfrastructure for Astronomy V*, Society of Photo-Optical Instrumentation Engineers (SPIE) Conference Series, Vol. 10707, edited by J. C. Guzman and J. Ibsen (2018) p. 1070711, arXiv:1806.09557 [astro-ph.IM].

[25] S. J. van der Walt, A. Crellin-Quick, and J. S. Bloom, Skyportal: An astronomical data platform, Journal of Open Source Software **4**, 1247 (2019).

[26] M. W. Coughlin, J. S. Bloom, G. Nir, S. Antier, T. J. du Laz, S. van der Walt, A. Crellin-Quick, T. Culino, D. A. Duev, D. A. Goldstein, B. F. Healy, V. Karambelkar, J. Lilleboe, K. M. Shin, L. P. Singer, T. Ahumada, S. Anand, E. C. Bellm, R. Dekany, M. J. Graham, M. M. Kasliwal, I. Kostadinova, R. W. Kiendrebeogo, S. R. Kulkarni, S. Jenkins, N. LeBaron, A. A. Mahabal, J. D. Neill, B. Parazin, J. Peloton, D. A. Perley, R. Riddle, B. Rusholme, J. van Santen, J. Sollerman, R. Stein, D. Turpin, A. Wold, C. Amat, A. Bonnefon, A. Bonnefoy, M. Flament, F. Kerkow, S. Kishore, S. Jani, S. K. Mahanty, C. Liu, L. Llinares, J. Makarison, A. Olliéric, I. Perez, L. Pont, and V. Sharma, A data science platform to enable time-domain astronomy, The Astrophysical Journal Supplement Series **267**, 31 (2023).

[27] I. Arcavi, The first hours of the gw170817 kilonova and the importance of early optical and ultraviolet observations for constraining emission models, The Astrophysical Journal Letters **855**, L23 (2018).

[28] S. S. Chaudhary, A. Toivonen, G. Waratkar, G. Mo, D. Chatterjee, S. Antier, P. Brockill, M. W. Coughlin, R. Essick, S. Ghosh, *et al.*, Low-latency gravitational wave alert products and their performance at the time of the fourth ligo-virgo-kagra observing run, Proceedings of the National Academy of Sciences **121**, e2316474121 (2024).

[29] B. P. Abbott, R. Abbott, T. D. Abbott, S. Abraham, F. Acernese, K. Ackley, C. Adams, R. X. Adhikari, V. B. Adya, C. Affeldt, M. Agathos, K. Agatsuma, N. Aggarwal, O. D. Aguiar, L. Aiello, A. Ain, P. Ajith, G. Allen, A. Allocca, M. A. Aloy, P. A. Altin, A. Amato, A. Ananyeva, S. B. Anderson, W. G. Anderson, S. V. Angelova, S. Antier, S. Appert, K. Arai, M. C. Araya, J. S. Areeda, M. Arène, N. Arnaud, S. Ascenzi, G. Ashton, S. M. Aston, P. Astone, F. Aubin, P. Aufmuth, K. AultONeal, C. Austin, V. Avendano, A. Avila-Alvarez, S. Babak, P. Bacon, F. Badaracco, M. K. M. Bader, S. Bae, P. T. Baker, F. Baldaccini, G. Ballardin, S. W. Ballmer, S. Banagiri, J. C. Barayoga, S. E. Barclay, B. C. Barish, D. Barker, K. Barkett, S. Barnum, F. Barone, B. Barr, L. Barsotti, M. Barsuglia, D. Barta, J. Bartlett, I. Bartos, R. Bassiri, A. Basti, M. Bawaj, J. C. Bayley, M. Bazzan, B. Bécsy, M. Bejger, I. Belahcene, A. S. Bell, D. Beniwal, B. K. Berger, G. Bergmann, S. Bernuzzi, J. J. Bero, C. P. L. Berry, D. Bersanetti, A. Bertolini, J. Betzwieser, R. Bhandare, J. Bidler, I. A. Bilenko, S. A. Bilgili, G. Billingsley, J. Birch, R. Birney, O. Birnholtz, S. Biscans, S. Biscoveanu, A. Bisht, M. Bitossi, M. A. Bizouard, J. K. Blackburn, C. D. Blair, D. G. Blair, R. M. Blair, S. Bloemen, N. Bode, M. Boer, Y. Boetzel, G. Bogaert, F. Bondu,

E. Bonilla, R. Bonnand, P. Booker, B. A. Boom, C. D. Booth, R. Bork, V. Boschi, S. Bose, K. Bossie, V. Bossilkov, J. Bosveld, Y. Bouffanais, A. Bozzi, C. Bradaschia, P. R. Brady, A. Bramley, M. Branchesi, J. E. Brau, T. Briant, J. H. Briggs, F. Brighenti, A. Brillet, M. Brinkmann, V. Brisson, P. Brockill, A. F. Brooks, D. D. Brown, S. Brunett, A. Buikema, T. Bulik, H. J. Bulten, A. Buonanno, D. Buskulic, C. Buy, R. L. Byer, M. Cabero, L. Cadonati, G. Cagnoli, C. Cahillane, J. Calderón Bustillo, T. A. Callister, E. Calloni, J. B. Camp, W. A. Campbell, M. Canepa, K. C. Cannon, H. Cao, J. Cao, E. Capocasa, F. Carbognani, S. Caride, M. F. Carney, G. Carullo, J. Casanueva Diaz, C. Casentini, S. Caudill, M. Cavaglià, F. Cavalier, R. Cavalieri, G. Cella, P. Cerdá-Durán, G. Cerretani, E. Cesarini, O. Chaibi, K. Chakravarti, S. J. Chamberlin, M. Chan, S. Chao, P. Charlton, E. A. Chase, E. Chassande-Mottin, D. Chatterjee, M. Chaturvedi, B. D. Cheeseboro, H. Y. Chen, X. Chen, Y. Chen, H. P. Cheng, C. K. Cheong, H. Y. Chia, A. Chincarini, A. Chiummo, G. Cho, H. S. Cho, M. Cho, N. Christensen, Q. Chu, S. Chua, K. W. Chung, S. Chung, G. Ciani, A. A. Ciobanu, and R. Ciolfi, Low-latency Gravitational-wave Alerts for Multimessenger Astronomy during the Second Advanced LIGO and Virgo Observing Run, Astrophys. J. **875**, 161 (2019), arXiv:1901.03310 [astro-ph.HE].

[30] R. Magee, D. Chatterjee, L. P. Singer, S. Sachdev, M. Kovalam, G. Mo, S. Anderson, P. Brady, P. Brockill, K. Cannon, T. D. Canton, Q. Chu, P. Clearwater, A. Codoreanu, M. Drago, P. Godwin, S. Ghosh, G. Greco, C. Hanna, S. J. Kapadia, E. Katsavounidis, V. Oloworaran, A. E. Pace, F. Panther, A. Patwary, R. D. Pietri, B. Piotrzkowski, T. Prestegard, L. Rei, A. K. Sreekumar, M. J. Szczepańczyk, V. Valsan, A. Viets, M. Wade, L. Wen, and J. Zweizig, First demonstration of early warning gravitational wave alerts (2021), arXiv:2102.04555 [astro-ph.HE].

[31] `https://rtd.igwn.org/projects/gwcelery/en/latest/`.

[32] `https://git.ligo.org/lscsoft/raven`.

[33] `https://gracedb.ligo.org/`.

[34] B. Moe, B. Stephens, and P. Brady, Gracedb—gravitational wave candidate event database (2016).

[35] S. Barthelmy, E. Burns, D. Dutko, M. Gibb, V. Gonzalez-Leon, T. Jaffe, R. Lorek, I. Martinez, T. McGlynn, J. Racusin, *et al.*, Introducing new gcn kafka broker and web site for transient alerts, GRB Coordinates Network **32419**, 1 (2022).

[36] C. Meegan, G. Lichti, P. Bhat, E. Bissaldi, M. S. Briggs, V. Connaughton, R. Diehl, G. Fishman, J. Greiner, A. S. Hoover, *et al.*, The fermi gamma-ray burst monitor, The Astrophysical Journal **702**, 791 (2009).

[37] S. D. Barthelmy, L. M. Barbier, J. R. Cummings, E. E. Fenimore, N. Gehrels, D. Hullinger, H. A. Krimm, C. B. Markwardt, D. M. Palmer, A. Parsons, *et al.*, The burst alert telescope (bat) on the swift midex mission, Space Science Reviews **120**, 143 (2005).

[38] C. Winkler, G. Di Cocco, N. Gehrels, A. Giménez, S. Grebenev, W. Hermsen, J. Mas-Hesse, F. Lebrun, N. Lund, G. Palumbo, *et al.*, The integral mission, Astronomy & Astrophysics **411**, L1 (2003).

[39] M. Tavani, G. Barbiellini, A. Argan, F. Boffelli, A. Bulgarelli, P. Caraveo, P. Cattaneo, A. Chen, V. Cocco, E. Costa, *et al.*, The agile mission, Astronomy & Astrophysics **502**, 995 (2009).

[40] P. Antonioli, R. T. Fienberg, F. Fleurot, Y. Fukuda, W. Fulgione, A. Habig, J. Heise, A. B. McDonald, C. Mills, T. Namba, and et al., Snews: the supernova early warning system, New Journal of Physics **6**, 114–114 (2004).

[41] S. Sachdev, S. Caudill, H. Fong, R. K. Lo, C. Messick, D. Mukherjee, R. Magee, L. Tsukada, K. Blackburn, P. Brady, *et al.*, The gstlal search analysis methods for compact binary mergers in advanced ligo's second and advanced virgo's first observing runs, arXiv preprint arXiv:1901.08580 (2019).

[42] S. A. Usman, A. H. Nitz, I. W. Harry, C. M. Biwer, D. A. Brown, M. Cabero, C. D. Capano, T. Dal Canton, T. Dent, S. Fairhurst, *et al.*, The pycbc search for gravitational waves from compact binary coalescence, Classical and Quantum Gravity **33**, 215004 (2016).

[43] T. Adams, D. Buskulic, V. Germain, G. M. Guidi, F. Marion, M. Montani, B. Mours, F. Piergiovanni, and G. Wang, Low-latency analysis pipeline for compact binary coalescences in the advanced gravitational wave detector era, Classical and Quantum Gravity **33**, 175012 (2016).

[44] Q. Chu, Low-latency detection and localization of gravitational waves from compact binary coalescences, PhD thesis, The University of Western Australia (2017).

[45] S. Klimenko, I. Yakushin, A. Mercer, and G. Mitselmakher, A coherent method for detection of gravitational wave bursts, Classical and Quantum Gravity **25**, 114029 (2008).

[46] T. Mishra, B. O'Brien, M. Szczepańczyk, G. Vedovato, S. Bhaumik, V. Gayathri, G. Prodi, F. Salemi, E. Milotti, I. Bartos, *et al.*, Search for binary black hole mergers in the third observing run of advanced ligo-virgo using coherent waveburst enhanced with machine learning, Physical Review D **105**, 083018 (2022).

[47] G. Ashton, E. Burns, T. Dal Canton, T. Dent, H.-B. Eggenstein, A. B. Nielsen, R. Prix, M. Was, and S. J. Zhu, Coincident detection significance in multimessenger astronomy, The Astrophysical Journal **860**, 6 (2018).

[48] C. Stachie, T. D. Canton, E. Burns, N. Christensen, R. Hamburg, M. Briggs, J. Broida, A. Goldstein, F. Hayes, T. Littenberg, *et al.*, Search for advanced ligo single interferometer compact binary coalescence signals in coincidence with gamma-ray events in fermi-gbm, arXiv preprint arXiv:2001.01462 (2020).

[49] R. Hamburg, C. Fletcher, E. Burns, A. Goldstein, E. Bissaldi, M. Briggs, W. Cleveland, M. Giles, C. Hui, D. Kocevski, *et al.*, A joint fermi-gbm and ligo/virgo analysis of compact binary mergers from the first and second gravitational-wave observing runs, The Astrophysical Journal **893**, 100 (2020).

[50] B. P. Abbott, R. Abbott, T. Abbott, M. Abernathy, F. Acernese, K. Ackley, C. Adams, T. Adams, P. Addesso, R. Adhikari, *et al.*, Gw150914: First results from the search for binary black hole coalescence with advanced ligo, Physical Review D **93**, 122003 (2016).

[51] B. Piotrzkowski, A. Baylor, and I. M. Hernandez, A joint ranking statistic for multi-messenger astronomical searches with gravitational waves, Classical and Quantum Gravity **39**, 085010 (2022).

[52] B. Zhang, The delay time of gravitational wave—gamma-ray burst associations, Frontiers of Physics **14**, 64402

(2019).

[53] A. L. Urban, *Monsters in the Dark: High Energy Signatures of Black Hole Formation with Multimessenger Astronomy*, Ph.D. thesis (2016).

[54] M.-A. Cho, *Low-Latency Searches for Gravitational Waves and Their Electromagnetic Counterparts with Advanced LIGO and Virgo*, Ph.D. thesis (2019).

[55] P. N. Bhat, C. A. Meegan, A. von Kienlin, W. S. Paciesas, M. S. Briggs, J. M. Burgess, E. Burns, V. Chaplin, W. H. Cleveland, A. C. Collazzi, *et al.*, The third fermi gbm gamma-ray burst catalog: the first six years, The Astrophysical Journal Supplement Series **223**, 28 (2016).

[56] T. Sakamoto, S. Barthelmy, W. Baumgartner, J. Cummings, E. Fenimore, N. Gehrels, H. Krimm, C. Markwardt, D. Palmer, A. Parsons, *et al.*, The second swift burst alert telescope gamma-ray burst catalog, The Astrophysical Journal Supplement Series **195**, 2 (2011).

[57] G. Vianello, D. Götz, and S. Mereghetti, The updated spectral catalogue of integral gamma-ray bursts, Astronomy & Astrophysics **495**, 1005 (2009).

[58] A. Ursi, M. Tavani, F. Verrecchia, M. Marisaldi, A. Argan, A. Trois, and P. Tempesta, A new agile mcal configuration to detect gamma-ray bursts and sub-threshold events in the multimessenger era, The Astrophysical Journal **871**, 27 (2019).

[59] D. Kocevski, E. Burns, A. Goldstein, T. Dal Canton, M. Briggs, L. Blackburn, P. Veres, C. Hui, R. Hamburg, O. Roberts, *et al.*, Analysis of sub-threshold short gamma-ray bursts in fermi gbm data, The Astrophysical Journal **862**, 152 (2018).

[60] K. M. Górski, E. Hivon, A. J. Banday, B. D. Wandelt, F. K. Hansen, M. Reinecke, and M. Bartelmann, HEALPix: A Framework for High-Resolution Discretization and Fast Analysis of Data Distributed on the Sphere, Astrophys. J. **622**, 759 (2005), arXiv:astro-ph/0409513 [astro-ph].

[61] A. Zonca, L. Singer, D. Lenz, M. Reinecke, C. Rosset, E. Hivon, and K. Gorski, healpy: equal area pixelization and spherical harmonics transforms for data on the sphere in python, Journal of Open Source Software **4**, 1298 (2019).

[62] Zonca and et al., Healpy documentation, `https://healpy.readthedocs.io/en/latest/index.html` (2022), accessed 22-March-2022.

[63] L.-V.-K. Collaboration, Ligo/virgo public alerts user guide, `https://emfollow.docs.ligo.org/userguide/tutorial/multiorder_skymaps.html` (2018), accessed 22-March-2022.

[64] A. Zhang, D. Veske, A. C. Oliveira, A. Sinha, M. Xu, S. Countryman, Z. Marka, and S. Marka, Search for coincident high-energy neutrinos and ligo-virgo-kagra gravitational waves with llama, in *American Astronomical Society Meeting Abstracts*, Vol. 56 (2024) pp. 324–05.

[65] S. Countryman, A. Keivani, I. Bartos, Z. Marka, T. Kintscher, R. Corley, E. Blaufuss, C. Finley, and S. Marka, Low-latency algorithm for multi-messenger astrophysics (llama) with gravitational-wave and high-energy neutrino candidates, arXiv preprint arXiv:1901.05486 (2019).

[66] A. Keivani, D. Veske, S. Countryman, I. Bartos, K. R. Corley, Z. Marka, and S. Marka, Multi-messenger gravitational-wave+ high-energy neutrino searches with ligo, virgo, and icecube, arXiv preprint arXiv:1908.04996 (2019).

[67] V. Connaughton, M. Briggs, A. Goldstein, C. Meegan, W. Paciesas, R. Preece, C. Wilson-Hodge, M. Gibby, J. Greiner, D. Gruber, *et al.*, Localization of gamma-ray bursts using the fermi gamma-ray burst monitor, The Astrophysical Journal Supplement Series **216**, 32 (2015).

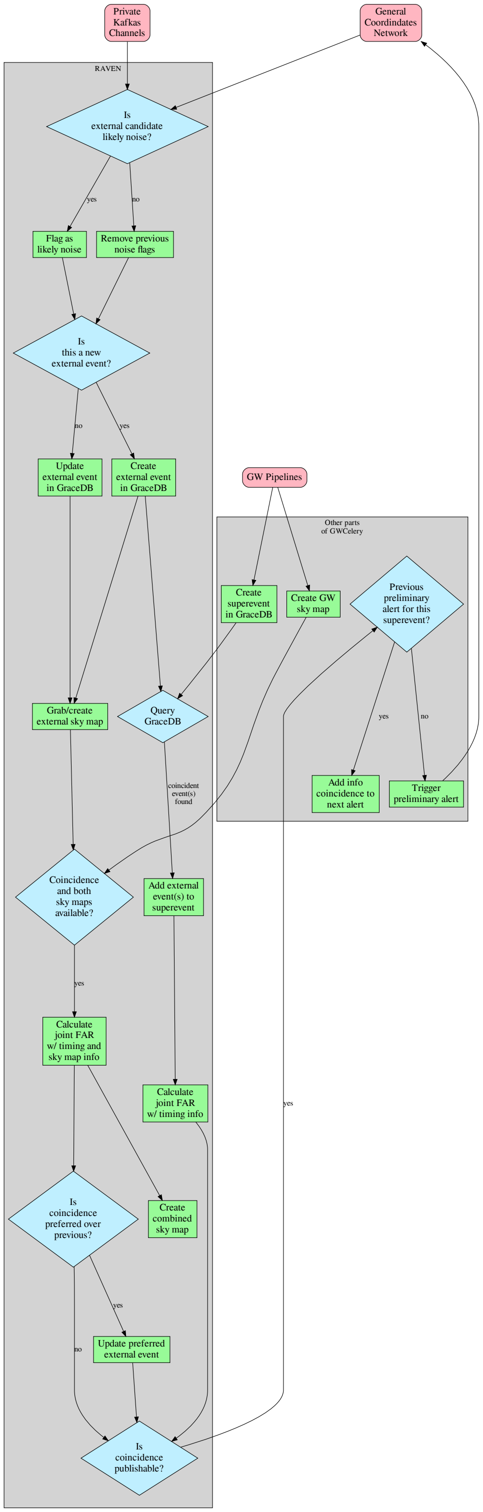

FIG. 1: A flowchart of the logic used for GW-GRB coincidences within the RAVEN pipeline. The flowchart shows the part of `gwcelery` where RAVEN is integrated and is used for low-latency joint GW-GRB coincidence searches. Note that the logic with SNEWS coincidence is identical without the use of sky maps.

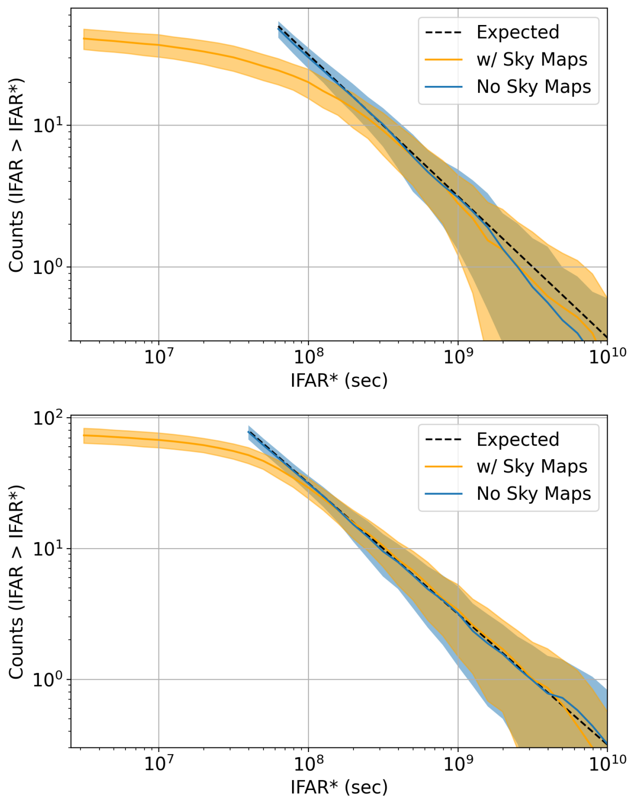

FIG. 2: Cumulative counts of the inverse joint false alarm rate (IFAR) calculated using sky maps (*orange*) and without sky maps (*blue*), with the top figure simulated from the untargeted Fermi/GBM search using eqn (1) and the bottom figure simulated from the targeted Fermi/GBM search using eqn (10). The colored regions represent a standard deviation of uncertainty around the mean, shown as a solid line. A skew is observed due to a number of instances with small overlap, as seen in figure 3. This skew is less pronounced in the targeted search because the low-significance GRB sky maps are less informative and more poorly localized.

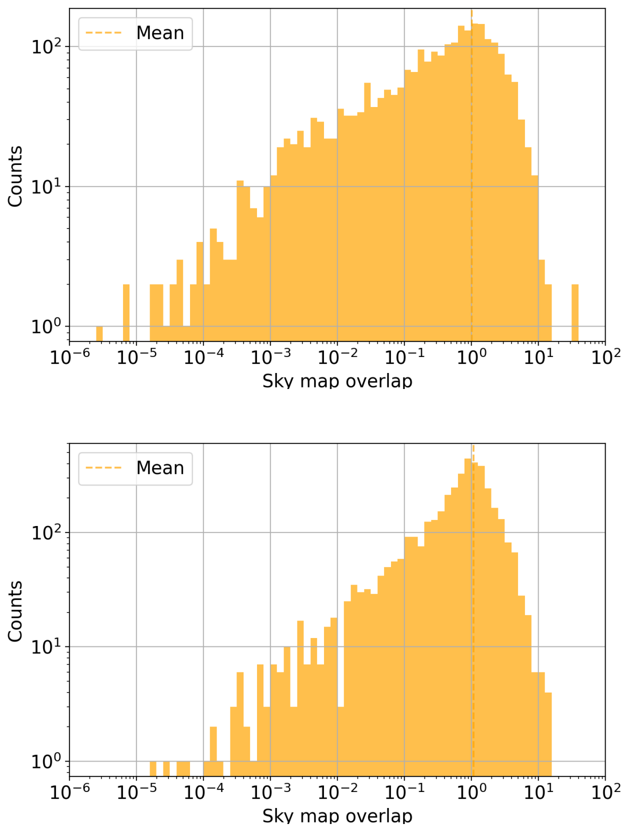

FIG. 3: Sky map overlap integral calculated with eqn (3) using Fermi/GBM-like sky maps consistent with each search, from the same simulation as figure 2. There are a number of very small overlap values due to astrophysically motivated localizations that are highly peaked and inconsistent with each other. Note that the mean of each method is consistent with 1.

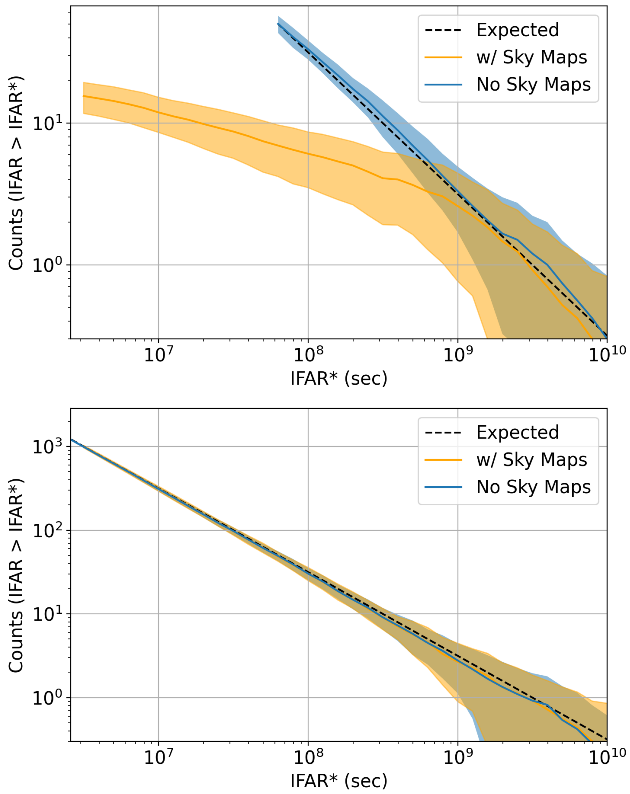

FIG. 4: Similar to figure 2, cumulative counts of the inverse joint false alarm rate (IFAR) calculated using sky maps (*orange*) and without sky maps (*blue*), with the top figure simulated from the untargeted *Swift*/BAT search using eqn (1) and the bottom figure simulated from the targeted *Swift*/BAT search using eqn (10). There is even greater skew than in figure 2 due to the large population of incredibly low sky map overlap values seen in figure 5.

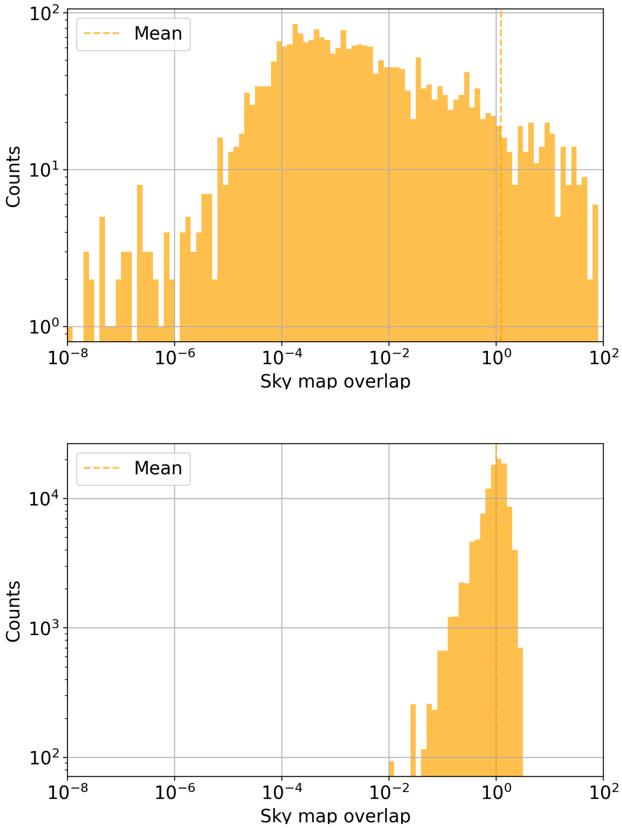

FIG. 5: Sky map overlap integral calculated with eqn (3) using *Swift*/BAT-like sky maps consistent with each search. Compared to figure 3, there are even lower overlap values due to the highly localized nature of *Swift* events. Note that, as in figure 3, the mean of each method is consistent with 1.

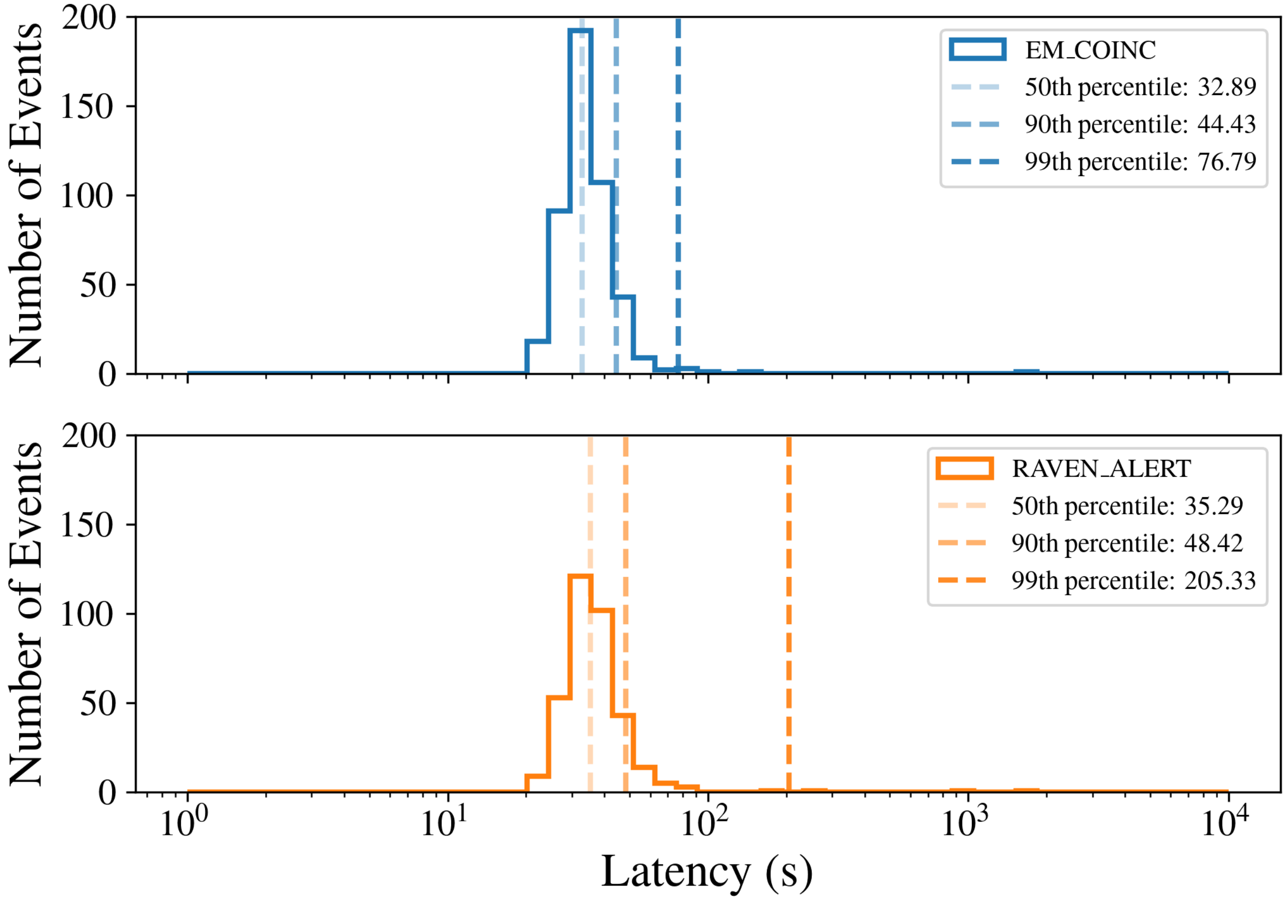

FIG. 6: Latency distributions for various alerts associated with the RAVEN workflow using the O3 Replay MDC. The top panel shows the latency distribution of the application of the `EM_COINC` alert label, indicating the moment a joint candidate was discovered. The bottom panel shows the latency distribution of the application of the `RAVEN_ALERT` label, indicating the moment a joint candidate passed the publishing conditions as described in Section III C. The 50th, 90th, and 99th percentiles are marked in each plot to highlight latency characteristics.